BBA - Molecular Basis of Disease 1865 (2019) 1113–1125

Contents lists available at ScienceDirect

BBA - Molecular Basis of Disease

journal homepage: www.elsevier.com/locate/bbadis

RhoC/ROCK2 promotes vasculogenic mimicry formation primarily through ERK/MMPs in hepatocellular carcinoma

Ji-Gang Zhang[a], Dan-Dan Zhang[b], Ying Liu[c], Juan-Ni Hu[a], Xue Zhang[a], Li Li[d], Wan Mu[a], Guan-Hua Zhu[a], Qin Li[a,*], Gao-Lin Liu[a,*]

[a] Department of Clinical Pharmacy, Shanghai General Hospital, Shanghai Jiao Tong University School of Medicine, No.100 Haining Road, Shanghai 200080, PR China
[b] Department of Pharmacy, Xinhua Hospital Affiliated to Shanghai Jiao Tong University School of Medicine, No.1665 Kongjiang Road, Shanghai 200092, PR China
[c] Department of Clinical Pharmacy, Zhongshan Hospital, Fudan University, No. 180 Fenglin Road, 200032 Shanghai, PR China
[d] Department of Pharmacy, The Eighth Affiliated Hospital of Sun Yat-Sen University, No 3025, Nanhai Road, 518033 Shenzhen, PR China

ARTICLE INFO

Keywords:
RhoC
ROCK1
ROCK2
Vasculogenic mimicry
Hepatocellular carcinoma

ABSTRACT

Vasculogenic mimicry (VM) results in the formation of an alternative circulatory system that can improve the blood supply to multiple malignant tumors, including hepatocellular carcinoma (HCC). However, the potential mechanisms of RhoC/ROCK in VM have not yet been investigated in HCC. Here, RhoC expression was upregulated in HCC tissues, especially the VM-positive (VM+) group, compared to noncancerous tissues ($P < 0.01$), and patients with high expression of RhoC had shorter survival times ($P < 0.001$). The knockdown of RhoC *via* short hairpin RNA (shRNA) in SK-Hep-1 cells significantly decreased VM formation and cell motility. In contrast, cell motility and VM formation were remarkably enhanced when RhoC was overexpressed in HepG2 cells. To further assess the potential role of ROCK1 and ROCK2 on VM, we stably knocked down ROCK1 or ROCK2 in MHCC97H cells. Compared to ROCK1 shRNA, ROCK2 shRNA could largely affect VM formation, cell motility and the key VM factors, as well as the epithelial-mesenchymal transition (EMT) markers *in vitro* and *in vivo*. Moreover, p-ERK, p-MEK, p-FAK, p-paxillin, MT1-MMP and MMP2 levels were clearly altered following the overexpression of RhoC, but ROCK2 shRNA had little effect on the expression of p-FAK, which indicated that RhoC regulates FAK/paxillin signaling, but not through ROCK2. In conclusion, our results show that RhoC/ROCK2 may have a major effect on VM in HCC *via* ERK/MMPs signaling and might be a potential therapeutic target for the treatment of HCC.

1. Introduction

Hepatocellular carcinoma (HCC) is the most common type of liver cancer due to the rising prevalence of hepatitis B and hepatitis C viral infections and an increase in the prevalence of (non-alcoholic) fatty liver disease caused by metabolic syndrome [1–4]. Cancer metastases, both intrahepatic and extrahepatic, are major contributors to the mortality of HCC patients. Vasculogenic mimicry (VM) results in the formation of a new blood supply system in aggressive tumor cells that express vascular cell markers and that line tumor vasculature. VM has been found in many malignant tumors, including HCC [5,6]. Thus, the inhibition of VM may be a potential treatment for HCC.

Recently, mounting evidence has demonstrated that the Rho GTPase family, one of the most well-characterized subfamilies, plays an important role in mediating HCC progression [7]. RhoC is involved in cancer progression, especially metastasis in various cancers, including HCC. The metastatic properties of RhoC have been clearly revealed in a RhoC knockdown cell model [8]. In addition, many research studies reported that overexpression of RhoC has been implicated in poor clinical prognosis due to the association with metastatic and aggressive features of HCC [7]. VM has been accepted as a new model of neovascular supply in aggressive tumors to enhance tumor growth and metastasis, which is related to poor prognosis of cancer patients [9]. However, RhoC as a therapeutic target for VM has not been documented.

Rho-associated coiled-coil containing kinases (ROCKs), which are key regulators of focal adhesion, actomyosin contraction, and cell motility, consist of two isoforms: ROCK1 and ROCK2. The overexpression of the two members of the ROCK family at the protein level has been demonstrated in testicular and bladder cancers [10,11]. ROCK1(−/−) mice display failure of the eyelid and ventral body wall closure and die soon after birth [12], while ROCK2(−/−) mice

* Corresponding authors.
E-mail addresses: liqin0626@hotmail.com (Q. Li), gaolinliu@aliyun.com (G.-L. Liu).

https://doi.org/10.1016/j.bbadis.2018.12.007
Received 28 July 2018; Received in revised form 6 November 2018; Accepted 5 December 2018
Available online 16 February 2019
0925-4439/

experience embryonic lethality due to intrauterine growth retardation and placental dysfunction [13], suggesting that the regulation and signaling of these two proteins may be divergent to a measurable degree. Recently, a handful of reports have utilized RNAi technology to singularly disrupt each ROCK paralog *in vitro* and have demonstrated unique roles for each protein in the control of actin-cytoskeleton dynamics and cell morphogenesis, migration, cell fate decisions, and extracellular matrix assembly [14,15]. Previously, our study [16] found that ROCK is involved in VM in an HCC cell line, implying that ROCK may be a new attractive target for the development of HCC therapeutics due to its ability to inhibit VM. However, the various roles of the two ROCK isoforms in VM are still unclear.

VM is a complex process involving extensive signaling pathways. VE-cadherin regulates EphA2 activity by mediating its phosphorylation through interactions with its membrane-bound ligand ephrin-A1 and, in doing so, activates the expression of PI3K, matrix metalloproteinases (MMP) 2 and membrane type 1 (MT1)-MMP [17]. Both MT1-MMP and MMP2 promote the cleavage of LAMC2 into promigratory γ2′ and γ2× fragments, which, in turn, stimulate migration, invasion, and VM in melanoma cells [18]. EMT is thought to be a crucial mechanism that regulates the initial steps of metastatic progression [19]. We have demonstrated that EMT is correlated with ROCK-induced VM and that ROCK is involved in numerous aspects of the VM process [16]. In addition, extracellular signal-regulated kinase (ERK) can promote VM though MT1-MMP and MMP2 [20]. Furthermore, phosphorylation of the cytoplasmic tyrosine kinase focal adhesion kinase (FAK) can activate the downstream protein paxillin, thereby enhancing VM development [21]. However, the molecular mechanism for therapeutic targeting of ROCK1 or ROCK2 to inhibit VM has not been documented.

In this study, we investigated the role of RhoC in HCC and the specific molecular mechanism for its interaction with ROCK isoforms.

2. Materials and methods

2.1. Tissue microarrays

In total, 80 cases of hepatocellular carcinoma tissues and adjacent nontumorous liver tissues were purchased from Shanghai Outdo Biotech Company (China). Three patients were excluded due to a lack of completed clinical and follow-up data. The complete clinical and pathological features of these patients were collected and summarized in Table 1. Detailed information is provided in the Supplementary Materials.

2.2. Materials: antibodies and cell lines

The antibodies used are presented in Supplementary Table S1. U0126 [22] or TBHQ [23] (Selleck Chemicals, Houston, TX, USA) were used to inhibit or activate p-ERK. Information of cell lines in Supplementary Table S2. Detailed information is presented in the Supplementary Materials.

2.3. Establishment of RhoC stably expressing cells and RhoC, ROCK1 or ROCK2 stable knockdown cells

The gene transfection *in vitro* is described in the Supplementary Materials. For lentivirus construction, the shRNA for RhoC and the negative control were cloned into the lenti knockdown vector pLenti-U6-shRNA-CMV- EGFP-T2A-Puro to produce Lenti-U6-shRNA (RhoC, ROCK1 or ROCK2)-CMV- EGFP-T2A-Puro. The core target sequences of the shRNA are presented in Supplementary Table S3. The full length of RhoC was cloned into the overexpression vector pLOV-EF1a-PuroR-CMV-EGFP-P2A-3FLAG to produce Lenti-EF1a-PuroR-CMV-EGFP-P2A-3FLAG-RhoC (Obio Technology Co., Ltd., Shanghai, China). The RhoC was amplified using the primers sets: 5′- ATGATGACGACAAATCTAG AGCCACCATGGCTGCAATCCGAAAG-3′ and 5′- TCGACGCCTAGGGCG GCCGCTCAGAGAATGGGACAGCCC-3′.

Table 1
Associations between VM and clinico-pathological characteristics in HCC.

Variant	No. of patients	Tissue sample		*P*-value
		VM− (%)	VM+ (%)	
Cases	77	50 (64.9)	27 (35.1)	
Age (years)				
≤60	62	42 (67.7)	20 (32.3)	0.252[a]
> 60	15	8 (53.3)	7 (46.7)	
Gender				
Male	63	42 (66.7)	21 (33.3)	0.351[a]
Female	14	8 (57.1)	6 (42.9)	
Tumor size (cm)				
≤3	35	22 (62.9)	13 (37.1)	0.456[a]
> 3	42	28 (66.7)	14 (33.3)	
Clinical stage				
I/II	42	34 (81.0)	8 (19.0)	0.006[a,*]
III/IV	35	16 (45.7)	19 (54.3)	
Invasion depth				
T1 + T2	40	30 (75.0)	10 (25.0)	0.046[a,*]
T3 + T4	37	20 (54.1)	17 (45.9)	
Lymph nodes metastasis				
N0 (negative)	46	37 (80.4)	9 (19.6)	0.001[a,*]
N1 (positive)	31	13 (41.9)	18 (58.1)	
Distant metastasis				
M0 (absent)	72	46 (63.9)	26 (36.1)	0.422[b]
M1 (present)	5	4 (80.0)	1 (20.0)	

[a] Chi-square test.
[b] Fisher's exact test.
* $P < 0.05$ indicates a significant association among the variables.

2.4. Immunohistochemistry (IHC) and scoring

Antibody dilutions are presented in Supplementary Table S1. Detailed information is provided in the Supplementary Materials.

2.5. Western blot analysis, cDNA generation, real-time qPCR and immunostaining

Antibody dilutions are presented in Supplementary Table S1, primer design is presented in Supplementary Table S4, and the experimental procedures were described in a previous study. All data analyses were performed in duplicate and some were repeated three times. Detailed information is presented in the Supplementary Materials.

2.6. Cell apoptosis, Matrigel tube formation assay, cell migration assay, and Matrigel invasion assay

All experimental procedures were described in a previous study. All data analyses were performed in duplicate and some were repeated three times. Detailed information is provided in the Supplementary Materials.

2.7. Mouse tumor model and tumor growth analysis

Female Balb/c nude mice (5 weeks old), purchased from Shanghai SLAC Laboratory Animal Co., LTD (Shanghai, China), were randomly divided into three groups: Control shRNA, ROCK1 shRNA or ROCK2 shRNA (n = 10 mice/group). Detailed information is provided in the Supplementary Materials.

2.8. Statistical analysis

The data are expressed as the mean ± standard error (S.E.). The differences between the two groups were compared with the *t*-test, χ^2 tests or Fisher's exact methods as appropriate. Overall survival (OS) was analyzed using the Kaplan-Meier method with the log-rank test. All statistical analyses were carried out using SPSS 19.0. *P*-values of < 0.05 were considered statistically significant.

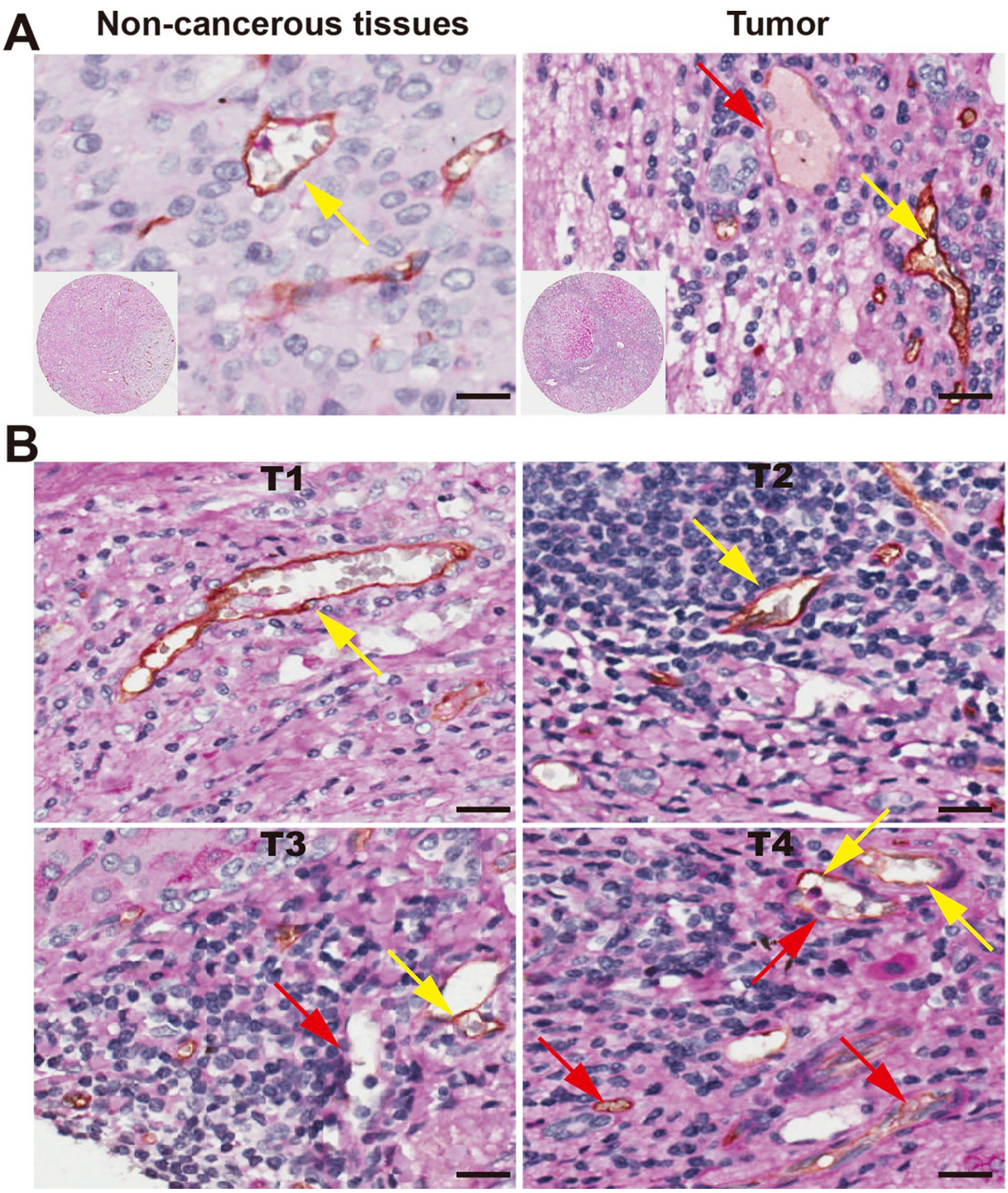

Fig. 1. CD34/PAS double staining for VM identification in clinical samples. (A) Evidence of VM in HCC tumor tissues. (B) VM is positively correlated with tumor stage. Endothelium-dependent vessels (yellow arrow) exhibited CD34-positive on their luminal surface, and positive reaction to PAS in their wall. VM channels (red arrow) made of HCC cells were positive for PAS staining, but negative for CD34. Original magnification 200×. The scales represent 50 μm.

3. Result

3.1. VM presented in HCC tissues

PAS/CD34 double staining was used to identify VM in HCC tissues. Endothelium-dependent vessels exhibited CD34+ on their luminal surface. Meanwhile, VM channels surrounded by HCC cells were positive for PAS staining, but negative for CD34 (Fig. 1, yellow arrow indicating blood vessel; red arrow indicates VM channels). Of 77 tumor tissue samples, VM channels were detected in 27 (35.1%) HCCs. Well-documented clinical data are presented in Table 1. As shown in Fig. 1A, VM channels were present in tumor tissues, but absent in corresponding noncancerous tissues. In addition, VM channels were positively correlated with clinical stage ($P = 0.006$; Fig. 1B; Table 1).

3.2. High RhoC expression is associated with poor clinical outcome in HCC patients

As shown in Table 2, of 77 tumor tissue samples, 45 (58.4%) HCC tissues had high RhoC expression, while only 11 (11.7%) of the noncancerous

Table 2
Protein expression of RhoC in HCC cancer tissues and adjacent normal tissues.

Tissue sample	No. of patients	RhoC		*P*-value
		Low (%)	High (%)	
Tumor	77	32 (41.6)	45 (58.4)	0.000*
Non-cancerous tissues	77	68 (88.3)	9 (11.7)	
VM−	50	32 (64.0)	18 (36.0)	0.021*
VM+	27	10 (37.0)	17 (63.0)	

RhoC expression was measured in tumor and non-cancerous tissues. RhoC was higher in tumor tissues, in VM+ tumor sample, especially, whereas lower in non-cancerous tissues. Data were analyzed using the Chi-squared test.
* $P < 0.05$ indicates statistical significance.

tissues had overexpressed RhoC. In the 77 HCC samples, the high-expression of RhoC could be detected in 18 of the 50 (36%) of the VM-negative (VM−) samples and in 17 of the 27 (63%) VM-positive (VM+) samples. These results suggest that RhoC expression is upregulated in HCC tissues, especially in the VM+ tissues compared to VM− tissues ($P = 0.021$). We then correlated RhoC expression with clinical-pathological parameters in the HCC patients. According to the localization of RhoC protein in the cell membrane, we concluded that RhoC was positively correlated with clinical stage ($P = 0.003$; Fig. 2A; Table 3) and lymph node metastasis ($P = 0.024$; Fig. 2B; Table 3). Meanwhile, there was no relationship between RhoC and age, sex, tumor size, invasion depth and distant metastasis. These data suggest a potential role of RhoC in HCC progression.

To test the predictive relationship between RhoC expression and patient prognosis, we conducted a Kaplan-Meier analysis. Patients with HCC were subdivided according to IHC scores. High RhoC expression was associated with an especially poor prognosis for HCC patients ($P = 0.0001$; Fig. 2C).

3.3. Correlations between the expression level of RhoC and the capacity of VM formation

To examine the involvement of RhoC in VM formation, the expression of RhoC and VM capacity was investigated in eight cell lines. As shown in Fig. 3A, the expression of RhoC was significantly higher in SK-Hep-1 cells and lower in HepG2 cells. In addition, SK-Hep-1 had the capacity for VM formation, while HepG2 cells failed to form any tubes or networks (Fig. 3B). These data indicate that HCC cells with higher expression of RhoC were more likely to form VM channels.

To understand the role of RhoC in HCC progression, we stably overexpressed RhoC (GFP RhoC) and control vector (GFP) in HepG2 cells (Fig. 3C) and transfected SK-Hep-1 cells with shRNA-1 and shRNA-2 to inhibit RhoC expression (Fig. 3D). Meanwhile, RhoC shRNA-1, rather than RhoC shRNA-2, has been used in subsequent experiments due to the excellent transfection efficiency. Next, we utilized flow cytometry to eliminate any misinterpretation due to cell apoptosis and found that neither the transfection of plasmid nor Y27632 significantly induced apoptosis of SK-Hep-1 and HepG2 cells (Fig. 3E, F).

3.4. RhoC promotes VM formation, cell migration and invasion in vitro

To further characterize the representative factors, such as ROCK1, ROCK2, VE-cadherin, Vimentin and E-cadherin mediating VM, Western blotting of whole cell lysates was performed. RhoC shRNA-1 could effectively inhibit the expression of ROCK1, ROCK2, VE-cadherin and Vimentin, and enhance the expression of E-cadherin in SK-Hep-1 cells (Fig. 4A, left panel; Fig. 4B, top panel; $^{*}P < 0.05$, $^{**}P < 0.01$ *vs.* Control shRNA). The expression of ROCK1, ROCK2, VE-cadherin and Vimentin were raised with the GFP RhoC treatment, and E-cadherin reduced, while the degree of upregulation was reduced when simultaneously treated with a ROCK inhibitor (Y27632 50 μM). (Fig. 4A, right panel; Fig. 4B, bottom panel; $^{\#}P < 0.05$, $^{\#\#}P < 0.01$, $^{\#\#\#}P < 0.001$ *vs.* GFP; $^{\blacktriangledown}P < 0.05$, $^{\blacktriangledown\blacktriangledown}P < 0.01$ *vs.* GFP RhoC).

A well-established 3D culture was used to illuminates whether RhoC mediates the morphological alterations of the HCC cells. As shown in Fig. 4C, a knockdown cell model (SK-Hep-1) failed to form typical pipe-like structures (Fig. 4C, left panel; Fig. 4D, left panel; $^{***}P < 0.001$ *vs.* Control shRNA;), but HepG2, with the overexpressing RhoC, led to the

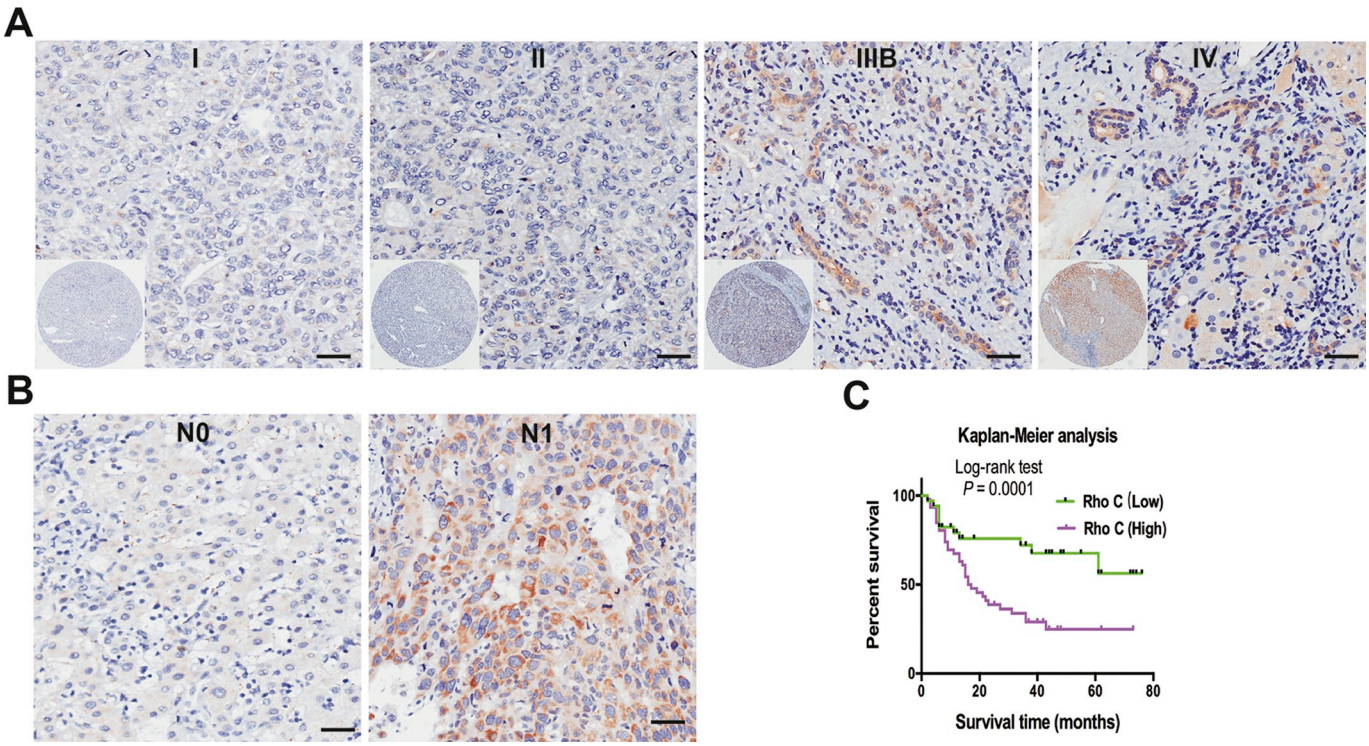

Fig. 2. Immunohistochemical staining for RhoC protein expression of HCC tissues with different clinical stages and with or without lymph nodes metastasis. (A) RhoC expression is positively correlated with advanced clinical stage. (B) RhoC expression is positively correlated with lymph node metastasis. (C) Patients with higher expression of RhoC possessed a worse prognosis. Original magnification 200×. The scales represent 50 μm.

Table 3
Associations between RhoC, ROCK and clinico-pathological characteristics in HCC.

Variant	No.	RhoC		*P*-value	ROCK1		*P*-value	ROCK2		*P*-value
		Low (%)	High (%)		Low (%)	High (%)		Low (%)	High (%)	
Cases	77	34 (44.2)	43 (55.8)		38 (49.4)	39 (50.6)		31 (40.3)	46 (59.7)	
Age (years)										
≤60	62	27 (43.5)	35 (56.5)	0.526[a]	29 (46.8)	33 (53.2)	0.264[a]	23 (37.1)	39 (62.9)	0.195[a]
> 60	15	7 (46.7)	8 (53.3)		9 (60.0)	6 (40.0)		8 (53.3)	7 (46.7)	0.299[a]
Gender										
Male	63	29 (46.3)	34 (53.7)	0.345[a]	30 (47.6)	33 (52.4)	0.364[a]	24 (38.1)	39 (61.9)	0.392[a]
Female	14	5 (35.7)	9 (64.3)		8 (57.1)	6 (42.9)		7 (50.0)	7 (50.0)	
Tumor size (cm)										
≤3	35	21 (60.0)	14 (40.0)	0.409[a]	14 (48.6)	21 (65.7)	0.143[a]	13 (37.1)	22 (62.9)	0.015[a,*]
> 3	42	23 (54.8)	19 (45.2)		22 (61.9)	18 (38.1)		18 (42.9)	24 (57.1)	
Clinical stage										
I/II	42	25 (59.5)	17 (40.5)	0.003[a,*]	23 (54.8)	19 (45.2)	0.209[a]	22 (52.4)	20 (47.6)	0.573[a]
III/IV	35	9 (25.7)	26 (74.3)		15 (42.9)	20 (57.1)		9 (25.7)	26 (74.3)	
Invasion depth										
T1 + T2	40	20 (50.0)	20 (50.0)	0.199[a]	19 (47.5)	21 (53.5)	0.456[a]	16 (40.0)	24 (60.0)	0.029[a,*]
T3 + T4	37	14 (37.8)	23 (62.2)		19 (51.4)	18 (48.6)		15 (40.5)	22 (59.5)	
Lymph nodes metastasis										
N0 (negative)	46	25 (54.3)	21 (45.7)	0.024[a,*]	25 (54.3)	21 (45.7)	0.389[a]	23 (50.0)	23 (50.0)	0.683[b]
N1 (positive)	31	9 (29.0)	22 (71.0)		15 (48.4)	16 (51.6)		8 (25.8)	23 (74.2)	
Distant metastasis										
M0 (absent)	72	33 (45.8)	39 (54.2)	0.089[b]	35 (48.6)	37 (51.4)	0.487[b]	29 (40.3)	43 (59.7)	
M1 (present)	5	1 (20.0)	4 (80.0)		3 (60.0)	2 (40.0)		2 (40.0)	3 (60.0)	

[a] Chi-square test.
[b] Fisher's exact test.
* $P < 0.05$ indicates a significant association among the variables.

opposite result. In additionally, ROCK inhibitor (Y27632 50 μM) decreased the degree of upregulation. (Fig. 4C, right panel; Fig. 4D, right panel; $^{\#\#\#}P < 0.001$ *vs.* GFP RhoC; $\blacktriangledown\blacktriangledown\blacktriangledown P < 0.001$ *vs.* GFP RhoC). These data indicate that RhoC significantly affects the formation of pipe-like structures *via* ROCK.

We then investigated cell migration and invasion due to its close relationship with VM formation. As shown in Fig. 4E and F, there was a significant difference in the speed of wound healing between the Control shRNA group and RhoC shRNA-1 group ($^{***}P < 0.001$ *vs.* 0 h; $^{\#\#\#}P < 0.001$ *vs.* 0 h). The cell invasion quantity was decreased in the RhoC shRNA-1 group compared with the Control shRNA group (Fig. 4G, left panel; Fig. 4H, left panel; $^{**}P < 0.01$ *vs.* Control shRNA). We also observed an increase in GFP RhoC transfected HepG2 cells compared to the GFP group and a decrease in the GFP RhoC cells treated with Y27632 (Fig. 4G, right panel; Fig. 4H, right panel; $^{\#\#\#}P < 0.001$ *vs.* GFP; $\blacktriangledown\blacktriangledown P < 0.01$ *vs.* GFP RhoC). These results indicate that RhoC/ROCK activation might lead to increased invasiveness and migration of HCC cells and that it could also play an important role in VM formation *in vitro*.

3.5. Different role of ROCK1 and ROCK2 on VM formation and cell motility in vitro

As shown in Table 3, both ROCK1 and ROCK2 (serine/threonine kinase downstream effectors) of RhoC were positively correlated with lymph node metastasis ($P = 0.012$; $P = 0.029$). Moreover, ROCK2 expression was positively correlated with clinical stage (Fig. 5A, B), which is consistent with RhoC, while ROCK1 was not (Supplemental Fig. S1A). Additionally, no relationship was found between ROCKs and age, sex, tumor size, invasion depth and distant metastasis. Kaplan-Meier analysis showed that high ROCK2 expression was associated with an especially poor prognosis for HCC patients ($P = 0.0014$; Fig. 5C), while ROCK1 was not ($P > 0.005$; Supplemental Fig. S1B).

To further demonstrate the potential role of ROCK1 or ROCK2 in VM formation, MHCC97H cells were stably transfected with either nontargeting (Control) shRNA or a panel of ROCK1 or ROCK2 shRNA plasmids. ROCK1 shRNA-2 (ROCK1 shRNA) and ROCK2 shRNA-4 (ROCK2 shRNA) has been used in subsequent experiments (Fig. 5D; $^{***}P < 0.001$ *vs.* Control shRNA; Supplemental Fig. S2), indicating that no cross-reactivity occurred between these two constructs.

To examine the effect of ROCK1 or ROCK2 shRNA on VM, parallel studies were performed with Y27632 50 μM (positive control). Compared to Control shRNA, ROCK2 shRNA and Y27632 50 μM could significantly inhibit VM formation (Fig. 5E; $^{*}P < 0.05$, $^{***}P < 0.001$ *vs.* Control shRNA), implying that the suppression of VM can mainly be attributed to the inhibition of ROCK2 rather than ROCK1. Cell proliferation assays showed that ROCK1 or ROCK2 shRNA did not affect cell growth ($P > 0.05$ *vs.* Control shRNA, Supplemental Fig. S3), confirming that inhibition of ROCK only affected HCC cell migration.

To further explore the distinctive effects of ROCK1 and ROCK2 on HCC cell motility, scratch wound and invasion assays were carried out. Compared to ROCK1 shRNA, ROCK2 shRNA and Y27632 50 μM significantly blocked the migration at 48 h, while ROCK1 shRNA failed to inhibit the migration (Fig. 5F; $^{**}P < 0.01$, $^{***}P < 0.001$ *vs.* 0 h), implying that ROCK1 has less of an effect on the inhibition of migration over a long period of time compared with ROCK2. A similar tendency was shown in the cell invasion results (Fig. 5G; $^{***}P < 0.001$ *vs.* Control shRNA). These findings demonstrated that ROCK2 plays the primary role in blocking migration and invasion.

To uncover the possible mechanism underlying the ROCK-mediated effect on VM, numerous key factors involved in VM were evaluated by real time-qPCR, Western blotting and immunofluorescence. Analyses of real-time qPCR (Supplemental Fig. S4) showed that ROCK2 shRNA significantly affected VE-cadherin and Twist1 mRNA levels, compared with Control shRNA, but ROCK1 shRNA did so only occasionally. VE-cadherin, PI3K, MMP2 and Vimentin, chosen for Western blotting and immunofluorescence, were significantly reduced in the ROCK2 shRNA and Y27632 50 μM groups compared with the Control shRNA group, but ROCK1 shRNA did not (Fig. 5H; $^{**}P < 0.01$, $^{***}P < 0.001$ *vs.* Control shRNA, and 5I). These results demonstrate that ROCK1 and ROCK2 have different roles in regulating the expression of key VM factors during the inhibition of VM and strongly imply that ROCK2 might exert the primary effect on VM.

3.6. Effects of ROCK1 and ROCK2 on VM formation in mouse xenografts

To further clarify the effect of ROCK1 and ROCK2 on tumor growth *in vivo*, a mouse xenografts experiment was performed according to the protocol shown in Fig. 6A. Ten days after the cells were injected, the

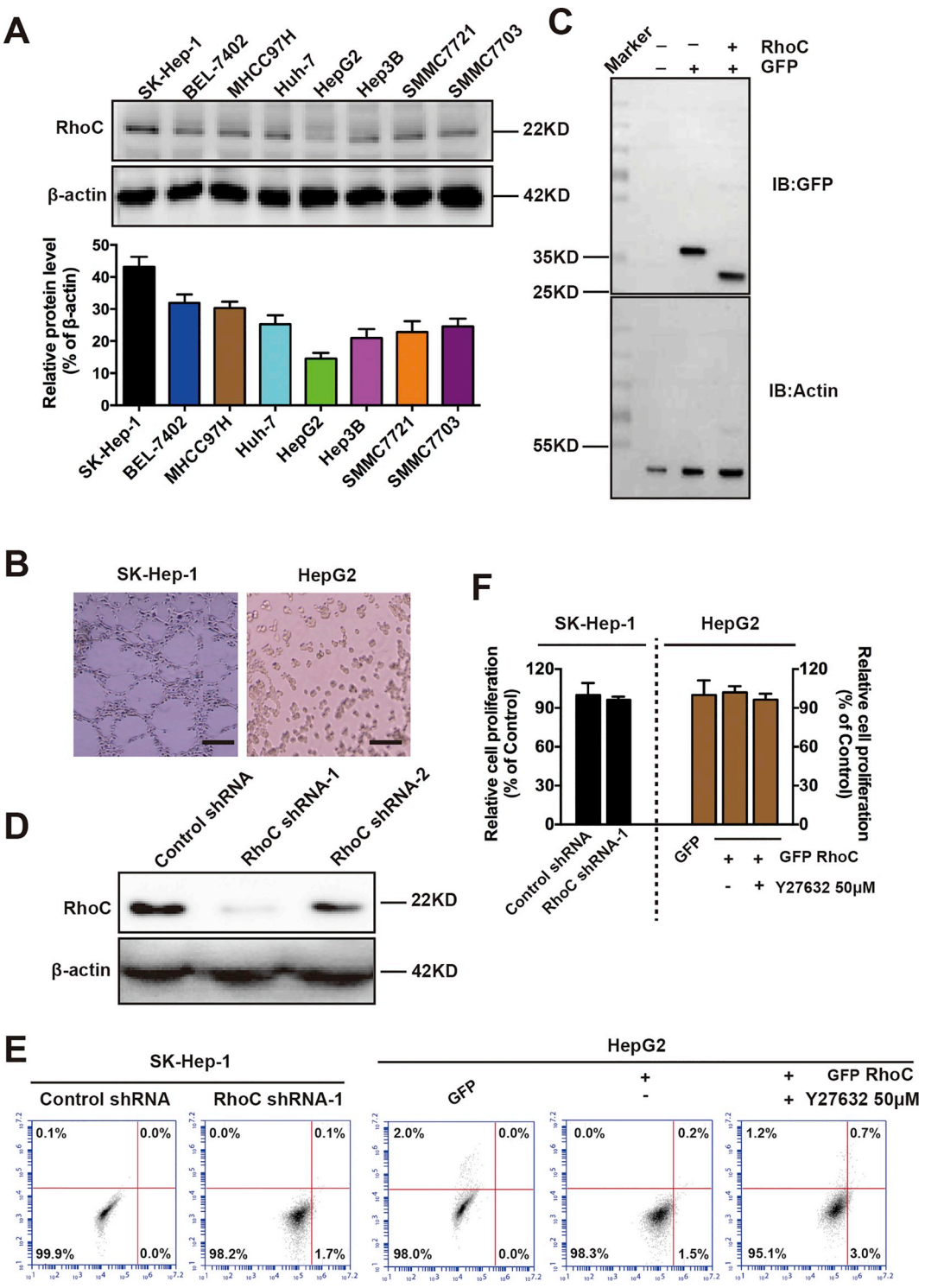

Fig. 3. RhoC expression level in HCC cell lines, introduction of SK-Hep-1 cells transfected with RhoC shRNA and RhoC with upregulation in HepG2 cells. (A) Western blotting was used to screen the level of RhoC in the HCC cell lines. SK-Hep-1 presented the highest level expression of RhoC, while HepG2 showed the lowest level. (B) Representative *in vitro* capillary network formation in SK-Hep-1 cells and HepG2 cells. Original magnification 100×. (C) Ectopic overexpression of GFP-ROCK2 fusion protein in HepG2 stable clones. (D) Western blotting analysis of a designed siRNA fragment specifically targeting RhoC in SK-Hep-1 cells. RhoC shRNA-1 (higher knockdown efficiency fragment) was chosen to perform the following experiment. (E) Apoptosis assay of SK-Hep-1 and HepG2 cells with different treatments were examined by flow cytometry. (F) Relative cell proliferation was calculated using the following equation: Relative cell proliferation (%) = (100-early apoptotic cells-late apoptotic cells) × 100%. The scales represent 50 μm.

right flank region of the mice contained palpable engrafted tumors. The engrafted tumors in the ROCK2 shRNA group (20 days after injection) and the ROCK1 shRNA group (30 days after injection) were significantly reduced in comparison with the Control shRNA group (Fig. 6B; C; $^{*}P < 0.05$, $^{**}P < 0.01$ *vs.* Control shRNA). Tumor death continued in the Control shRNA and ROCK1 shRNA group (Fig. 6D). These results demonstrated that ROCK2 may play the major role in regulating and preventing tumor growth.

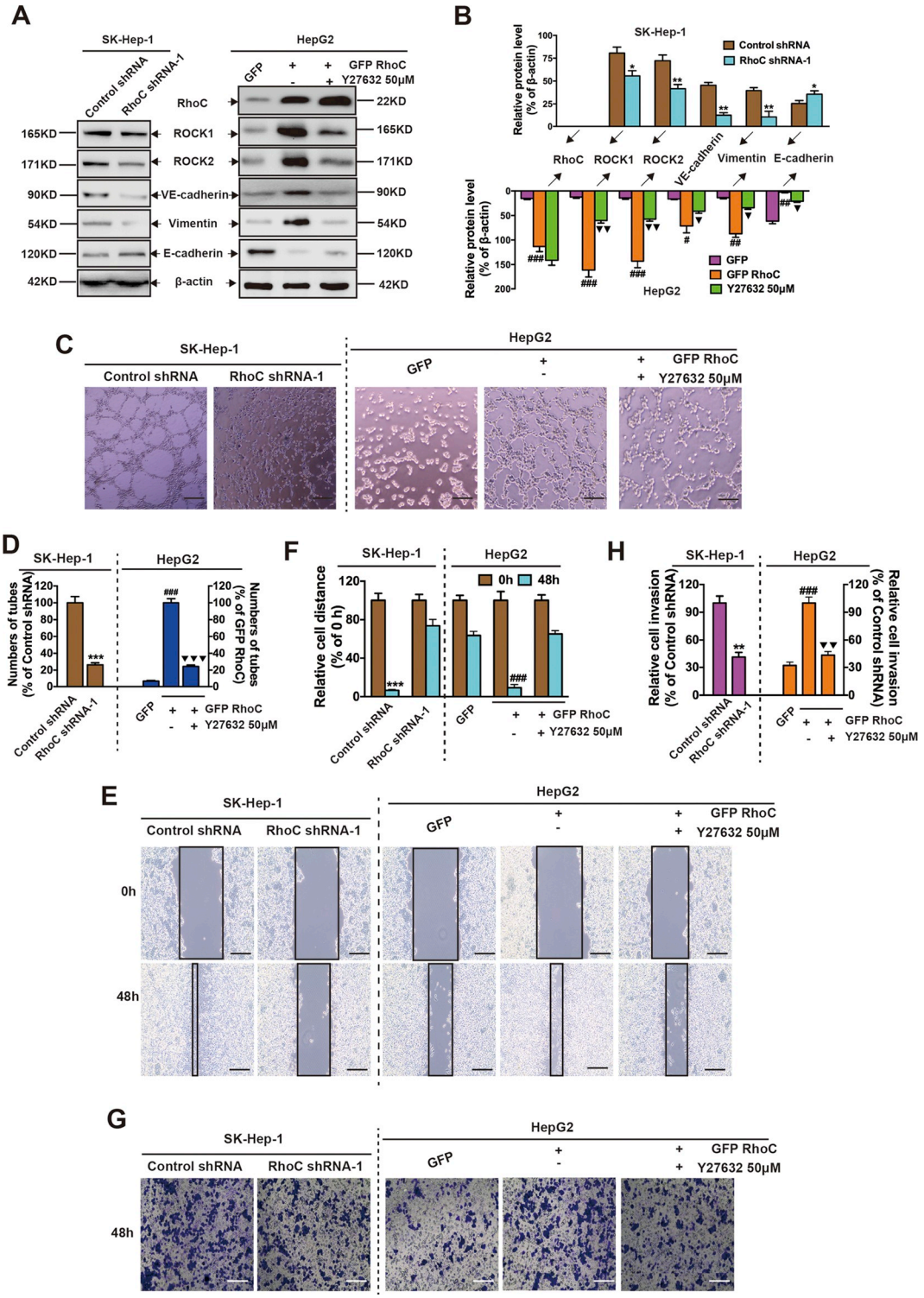

Fig. 4. RhoC promotes VM formation *in vitro*. (A) Western blotting was performed to evaluate the effect of RhoC on the expression of VM signaling-related markers and EMT markers. (B) The relative protein level was quantified using ImageJ (**$P < 0.01$ *vs.* control shRNA; $^{\#}P < 0.05$, $^{\#\#}P < 0.01$, $^{\#\#\#}P < 0.001$ *vs.* GFP; $^{\blacktriangledown}P < 0.05$, $^{\blacktriangledown\blacktriangledown}P < 0.01$ *vs.* GFP RhoC). (C) Representative *in vitro* capillary network formation of SK-Hep-1 cells treated with control shRNA or RhoC shRNA and HepG2 cells treated with GFP, GFP RhoC or GFP RhoC + Y27632 50 μM (original magnification, 100×). (D) Quantitative analysis of the mean number of tube-like structures formed from six randomly chosen areas in 3D cultures using ImageJ (***$P < 0.001$ *vs.* Control shRNA; $^{\#\#\#}P < 0.001$ *vs.* GFP; $^{\blacktriangledown\blacktriangledown\blacktriangledown}P < 0.001$ *vs.* GFP RhoC). Cells with different treatment were plated, incubated for 8 h, and then scratched for 0 and 48 h incubation (E; original magnification, 100×) or plated in Corning Transwell inserts coated with Matrigel for 48 h invasion (G; original magnification, 200×). The relative migration (F; ***$P < 0.001$ *vs.* 0 h; $^{\#\#\#}P < 0.001$ *vs.* 0 h) and invasion (H; **$P < 0.01$ *vs.* Control shRNA; $^{\#\#}P < 0.01$, $^{\#\#\#}P < 0.001$ *vs.* GFP RhoC; $^{\blacktriangledown\blacktriangledown}P < 0.01$ *vs.* GFP RhoC) were quantified. The data are expressed as the mean ± S.E. of three independent experiments. The scales represent 50 μm.

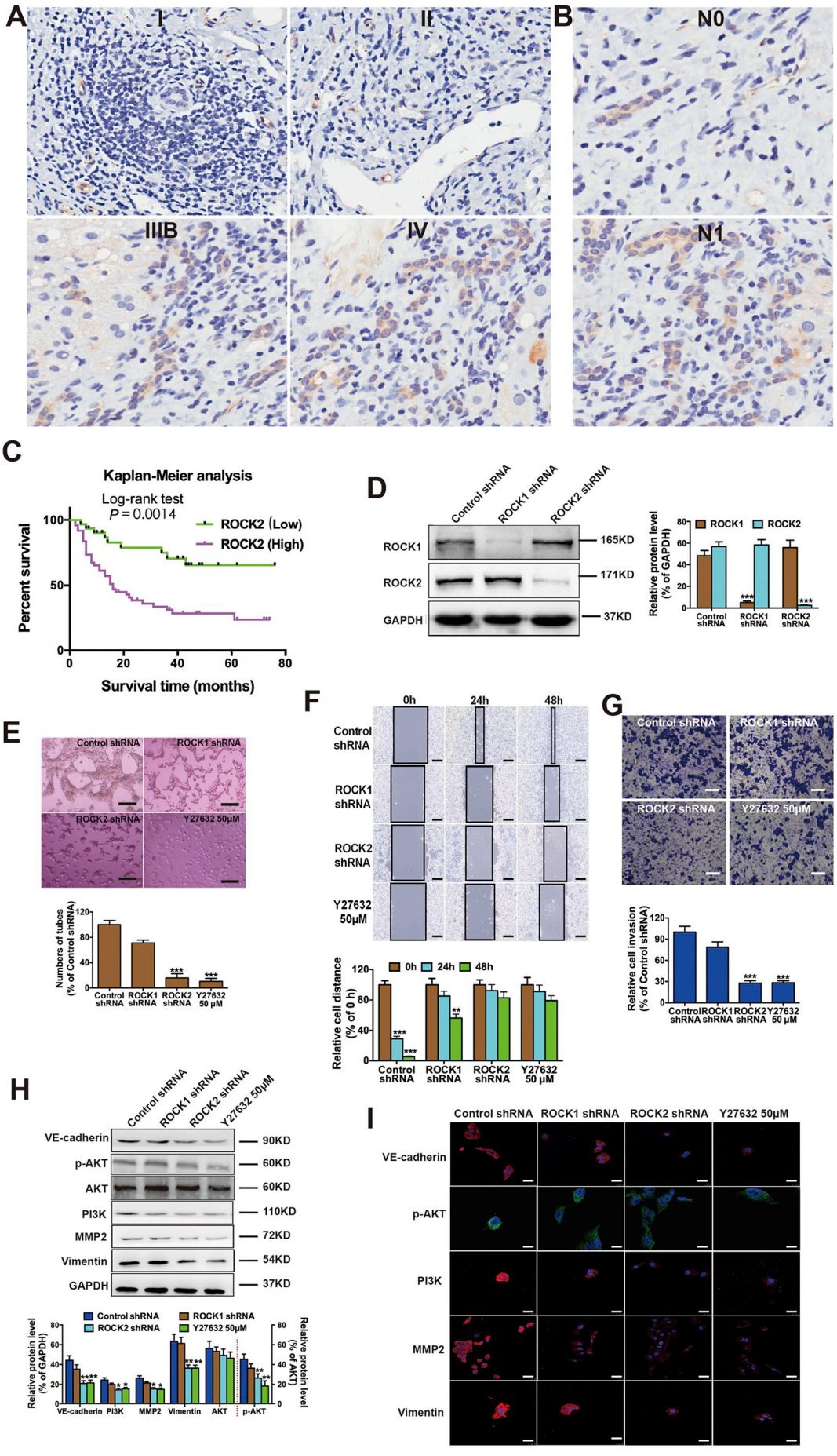

(caption on next page)

Fig. 5. ROCK2 primarily promotes VM formation *in vitro*. ROCK2 expression is positively correlated with (A) advanced clinical stage and (B) lymph node metastasis. (C) Patients with higher expression of ROCK2 possessed a worse prognosis. (D) Western blotting analysis of ROCK expression in stable ROCK knockdown MHCC97H cells. Quantified using ImageJ (***$P < 0.001$ *vs.* Control shRNA). (E) Representative *in vitro* capillary network formation of MHCC97H cells treated with control shRNA, ROCK1 shRNA or ROCK2 shRNA (original magnification, 100×, Scale bars: 50 μm). Quantitative analysis of the mean number of tube-like structures. (***$P < 0.001$ *vs.* Control shRNA). Cells from the control shRNA group treated with or without 50 μM Y27632, ROCK1 shRNA group, or ROCK2 shRNA group were plated, incubated for 8 h, and then scratched for 0, 24 and 48 h incubation (F; **$P < 0.01$, ***$P < 0.001$ *vs.* 0 h; original magnification, 100×; Scale bars: 50 μm) or plated in Corning Transwell inserts coated with Matrigel for 48 h invasion (G; ***$P < 0.001$ *vs.* Control shRNA; original magnification, 200×; Scale bars: 50 μm). Western blotting (H; *$P < 0.05$ and **$P < 0.01$ *vs.* Control shRNA) and immunofluorescence (I; original magnification, 200×; Scale bars: 50 μm) was performed to evaluate the effect of ROCKs on the *in vitro* expression of VE-cadherin, PI3K, MMP2 and Vimentin. The data are expressed as the mean ± S.E. of three independent experiments.

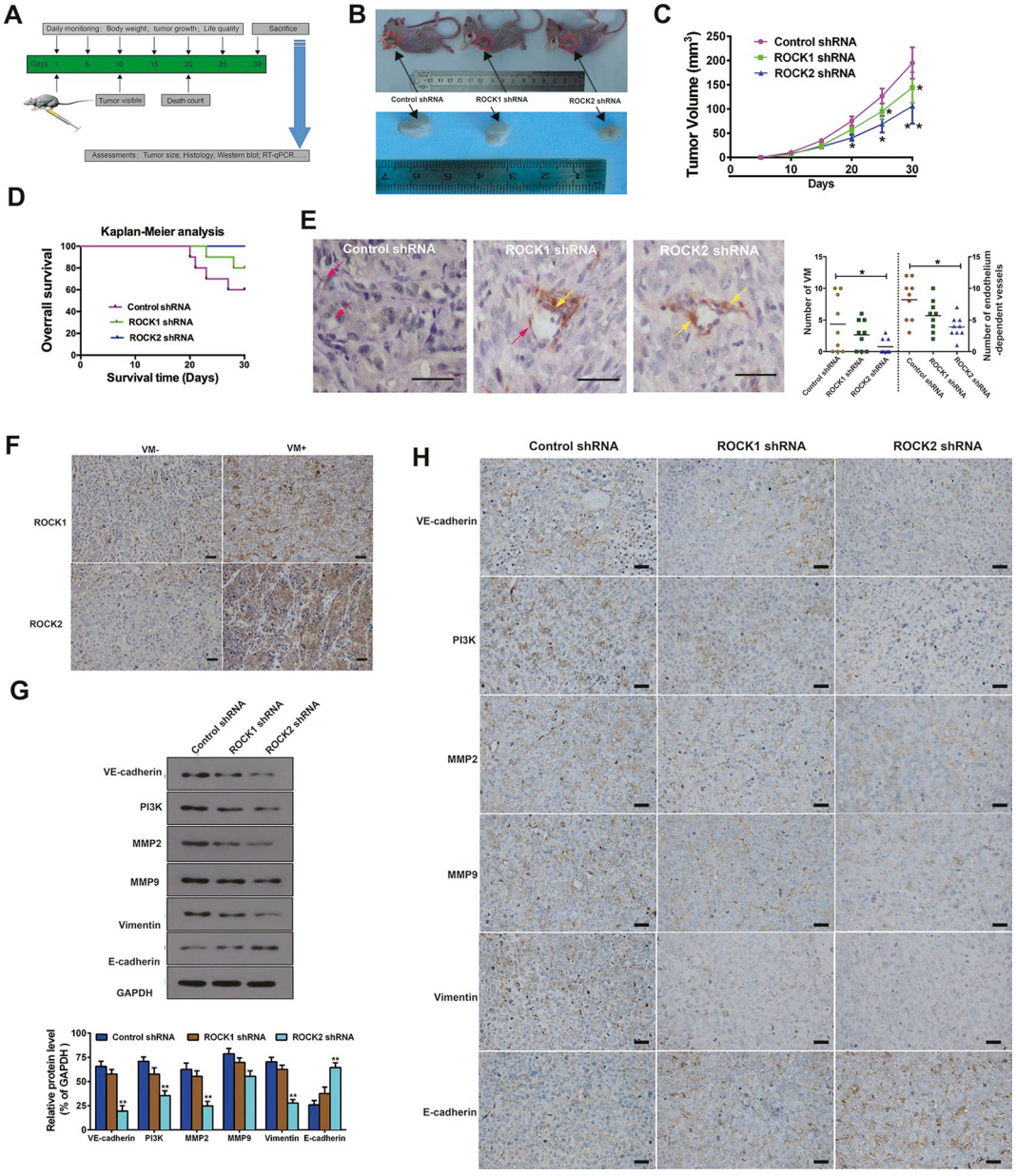

Fig. 6. ROCK2 primarily promotes VM formation *in vivo*. (A) Experimental procedure for the different effects of ROCK isoforms on VM formation in mouse xenografts. Nude mice that were injected subcutaneously in the right flank with control shRNA-, ROCK1 shRNA-, or ROCK2 shRNA-expressing MHCC97H cells. A total of 10 days after the cells were injected, the right flank region of the mice contained palpable engrafted tumors. Tumor death emerged and was counted from day 15. Sacrifice was performed on day 30. (B) Selected nude mice and tumors from the control, ROCK1, and ROCK2 shRNA groups 30 days after injection. (C) A plot showing the volume of the tumors in the different groups of mice (*$P < 0.05$ and **$P < 0.01$ *vs.* Control shRNA). (D) Nude mice with lower expression of ROCK2 possessed a better prognosis. (E) CD34/PAS double staining for VM identification in each group (original magnification, 200×; Scale bars: 50 μm; *$P < 0.05$ *vs.* Control shRNA). (F) Representative immunohistochemical staining of the ROCK proteins in VM+ specimen and VM− specimen (original magnification, 200×; Scale bars: 50 μm). Western blotting (G; *$P < 0.05$ and **$P < 0.01$ *vs.* Control shRNA) and immunohistochemical staining (H) were performed to evaluate the effect of ROCKs on the *in vivo* expression of VE-cadherin, PI3K, MMP2 and Vimentin (original magnification, 200×; Scale bars: 50 μm). The data are expressed as the mean ± S.E. of three independent experiments.

To further characterize the correlation between ROCK1/ROCK2 and VM and to clarify the respective roles of ROCK1 and ROCK2 in VM, ROCK1 and ROCK2 expression was examined *via* IHC staining. It was found that the endothelium-dependent vessels (yellow arrow) and the VM (red arrow) in the ROCK2 group decreased when compared to the Control shRNA group (Fig. 6E, $^{*}P < 0.05$ *vs.* Control shRNA). The tumors in the Control shRNA group were divided into VM+ and VM− groups based on PAS/CD34 staining scores. As shown in Fig. 6F, ROCK expression in the VM+ group was significantly stronger than in the VM− group. Furthermore, ROCK2 expression was significantly positive compared with ROCK1 expression in VM+ group, implying that the association between ROCK2 and VM+ was stronger than the association between ROCK1 and VM+. Taken together, all of the data described above indicate that ROCK2 may play a primary role in the formation of VM *in vivo*.

To further test the regulation of VM signaling-related markers and EMT markers mediated by the knockdown of ROCK1 or ROCK2, Western blotting and immunohistochemistry were carried out on the tumor tissue from the nude mice. It was found that the expression of VE-cadherin, PI3K, MMP2, MMP9, Vimentin and E-cadherin was more significantly regulated in ROCK2 shRNA groups compared with the Control shRNA group, while not in the ROCK1 shRNA group (Fig. 6G, $^{**}P < 0.01$ *vs.* Control shRNA; 6H), implying that the inhibition of ROCK2 could effectively block VM, probably by downregulating key VM factors and reducing the occurrence of EMT. This is consistent with the results *in vitro*.

3.7. RhoC/ROCK2 promotes VM formation via ERK/MMP signaling pathways

We demonstrated that overexpression of RhoC significantly induced p-ERK, p-FAK, and p-paxillin levels. Meanwhile, expression of MT1-MMP and MMP2, which are downstream of p-ERK and play very important roles in metastasis and VM, was also upregulated (Fig. 7A; Supplemental Fig. S5A). However, the expression of MMP9 was not influenced. Furthermore, knockdown of ROCK2 significantly reduced p-ERK and p-MEK, but only slightly affected the expression of p-FAK and p-paxillin levels (Fig. 7B; Supplemental Fig. S5B). Expression of VE-cadherin, MT1-MMP, MMP2 and Vimentin decreased and E-cadherin increased following U0126 (20 μM) treatment (Fig. 7C; Supplemental Fig. S5C). The opposite results occurred after TBHQ (250 μM) stimulation (Fig. 7D; Supplemental Fig. S5D). To investigate whether RhoC/ROCK2 influence VM formation through the ERK signaling pathway, cells with overexpression of RhoC or cells with silenced ROCK2 were cultured on Matrigel in the presence of the p-ERK inhibitor U0126 or p-ERK activator TBHQ. Treatment with 10 and 20 μM U0126 for 24 h effectively impaired VM formation (Fig. 7E, F; $^{\#\#}P < 0.01$ and $^{\#\#\#}P < 0.001$ *vs.* GFP; $^{\blacktriangledown\blacktriangledown}P < 0.01$ and $^{\blacktriangledown\blacktriangledown\blacktriangledown}P < 0.001$ *vs.* GFP RhoC), while 100 and 250 μM TBHQ promoted VM formation (Fig. 7G, H; $^{*}P < 0.05$, $^{**}P < 0.01$ and $^{***}P < 0.001$ *vs.* ROCK2 shRNA). Since the ERK/MMP signaling pathways have been recognized as key in the regulation of VM and angiogenesis [20], our findings suggest that RhoC/ROCK2 acts, at least in part, *via* these cellular pathways to promote these processes in HCC.

4. Discussion

Currently, the presence of VM is reported to be associated with a high tumor grade, short survival, tumor invasion, and metastasis [24,25], suggesting that VM may play a vital role in the deterioration of HCC patients. As the most well-characterized Rho subfamily, RhoC has been implicated in poor clinical prognosis due to its association with metastatic and aggressive features of HCC and is likely to be a potential activator of VM [7]. ROCK isoforms, ROCK1 and ROCK2, may play distinct, and sometimes opposing roles in HCC cells [26–29].

VM is associated with high tumor grade, invasion and metastasis, and short survival in patients with HCC [30]. We initially examined VM in tissue samples and confirmed VM channels were present in tumor tissues, but absence in corresponding noncancerous tissues (Fig. 1), confirming VM exist in HCC. Moreover, VM channels were positively correlated with clinical stage in HCC (Table 1). In addition, we found that RhoC expression was positively correlated with VM, ROCK2, clinical stage and lymph node metastasis (Tables 2, 3), and high RhoC expression was associated with poor clinical outcome in HCC patients (Fig. 2). Together, these findings demonstrated that RhoC expression, positively correlated with VM, could be an independent prognostic marker for HCC.

ROCKs might be potential targets for the suppression of VM [16]. However, the upstream modulator has not been clarified. Our evidence shows that SK-Hep-1 cells (higher RhoC expression) had the capacity for VM formation, while HepG2 cells (lower RhoC expression) did not (Fig. 3B). Meanwhile, the process of VM formation was reversed *via* silencing RhoC in SK-Hep-1 cells and upregulating RhoC in HepG2 cells (Fig. 4C). We investigated the role of ROCK1 and ROCK2 in the inhibition of VM *in vitro* and *in vivo*. Interestingly, according to the results of the tumor staining (Fig. 6E, F), the association between ROCK2 knockdown and VM was more significant than the association between ROCK1 knockdown and VM. More importantly, ROCK2 shRNA could significantly inhibit VM *in vitro* and *in vivo*, whereas ROCK1 shRNA could not (Figs. 5C, 6E), implying that ROCK inhibition, mainly the downregulation of ROCK2, could successfully block VM. These data suggested that RhoC/ROCK2 overexpression might lead to poor prognosis in HCC *via* promotion of VM.

Metastasis occurs when the tumor cells infiltrate the surrounding tissue, invade the blood vessels, and leave the bloodstream at a different site. Blocking cell invasion and migration is regarded as an effective therapy for HCC. Hakem et al. [31] reported that RhoC was dispensable for embryogenesis and tumor initiation but essential for metastasis. Our evidence showed that the speed of cell migration and the cell invasion quantity was decreased in RhoC-silenced SK-Hep-1 cells compared with the Control shRNA group (Fig. 4E left panel; Fig. 4G left panel). In contrast, we observed an increase in GFP RhoC transfected HepG2 compared to GFP control (Fig. 4E right panel; 4G right panel). As shown in Fig. 5D, E, ROCK2 shRNA showed a more significant and persistent effect than both Control shRNA and ROCK1 shRNA. In light of our migration and invasion findings, we believe that RhoC/ROCK2 modulates the metastatic nature of HCC. Taken together, these data suggest that RhoC/ROCK2 might inhibit VM formation *via* reducing the mobility and metastasis of HCC cells.

In addition to VM and cell mobility, cell apoptosis and proliferation are indispensable for liver cancer development. We observed no significant changes in the monolayer growth rate for overexpressed RhoC or RhoC siRNA transfectants with Control shRNA (Fig. 3E, F), supported by some other researchers Xu et al. [32]. Our present study evaluated tumor size following the injection of nude mice with ROCK1 or ROCK2 shRNA-expressing MHCC97H cells. We report that knockdown of either ROCK paralog results in a significant reduction in HCC tumor volume (Figs. 6B, 3C). Moreover, ROCK2 shRNA could inhibit the increase in tumor size compared to Control shRNA and ROCK1 shRNA (Figs. 6B, 3C). This demonstrates that RhoC/ROCK2 may play an early and primary role in inhibiting cell proliferation, and that RhoC/ROCK2 will be an effective target for the treatment of HCC.

As the key signaling pathway of VM, the regulation of several molecules including the colocalization of VE-cadherin, the activation of PI3K by EphA2 and the subsequent induction and activation of MMP2 and MMP9 [33], as well as key factors related to EMT could decrease migration and invasion and may ultimately result in the inhibition of VM [34]. Based on a previous study, we tested the expression of those key factors related to VM *in vitro* and *in vivo*. Compared to Control shRNA, RhoC shRNA could effectively inhibit the expression of VE-

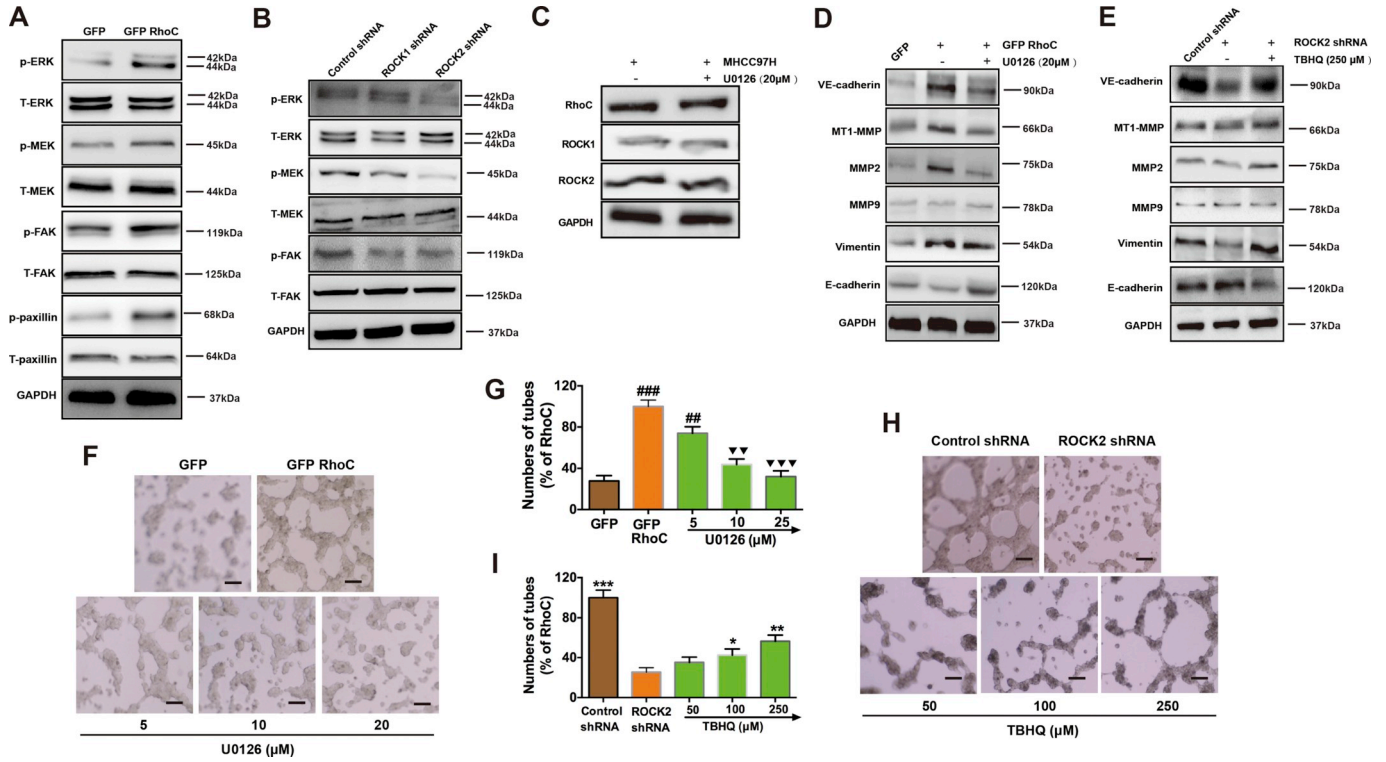

Fig. 7. RhoC/ROCK2 promoted VM *via* ERK/MMP signaling pathways. (A) p-ERK, p-MEK, p-FAK, and p-paxillin, and expression of MT1-MMP and MMP2, increased markedly following overexpression of RhoC. (B) Compared to ROCK1, p-ERK and p-MEK decreased markedly following suppression of ROCK2, while expression of p-FAK was not significantly affected. (C) MEK inhibitor (U0126) had no effect on RhoC/ROCK activation. Different influence of key VM factors and EMT markers using specified concentrations of U0126 (D) and TBHQ (E). Treatment with U0126 notably impaired VM formation in a dose-dependence manner (F, G: $^{\#\#}P < 0.01$, $^{\#\#\#}P < 0.001$ *vs.* GFP; $^{\blacktriangledown\blacktriangledown}P < 0.01$, $^{\blacktriangledown\blacktriangledown\blacktriangledown}P < 0.001$ *vs.* GFP RhoC). TBHQ (100 and 250 μM) notably stimulated VM formation (H, I: $^{*}P < 0.05$, $^{**}P < 0.01$, $^{***}P < 0.001$ *vs.* ROCK2 shRNA). Scale bars: 50 μm; original magnification, 100×. The data are expressed as the mean ± S.E. of three independent experiments. T: total. p: phosphorylation.

cadherin and Vimentin and increase E-cadherin in SK-Hep-1 cell (Fig. 4A, left panel; Fig. 4B, top panel), indicating that downregulation of the expression of RhoC markedly impeded EMT progression [35]. Conversely, the expression of VE-cadherin and Vimentin increased with the treatment of GFP RhoC (Fig. 4A, right panel; Fig. 4B, below panel), and decreased after simultaneously treated with a ROCK inhibitor (Y27632 50 μM), suggesting that RhoC significantly affects the formation of pipe-like structures *via* ROCK.

The results in Fig. 5F and G showed that ROCK2 shRNA could deplete the expression of VE-cadherin, PI3K, MMP2 and Vimentin compared with the Control shRNA. The evidence *in vivo* showed a consistent trend (Fig. 6G, H). Interestingly, ROCK could not affect the expression of MMP9, consistent with our previous results [16]. More importantly, the results from the ROCK2 shRNA group were more significant than those from the ROCK1 shRNA group both *in vivo* and *in vitro*, suggesting that ROCK2 could effectively block invasion and migration, and even inhibit VM, by downregulating the expression of key factors involved in VM. Thus, ROCK2 may be regarded as the primary regulator in the inhibition of VM.

MMP2 exerts a strong proteolytic effect on the extracellular matrix [36,37]. MT1-MMP, also known as MMP14, can enhance collagen IV degradation by forming a complex with the tissue inhibitor of metalloproteinase 2 and activating pro-MMP2 [38,39]. Previous reports show that p-ERK increases VM formation and involves the elevation of MMP levels [20,40]. We found that p-ERK, MT1-MMP and MMP2 levels clearly increased or decreased following overexpression of RhoC or inhibition of ROCK2 and reversed after being disposed of p-ERK activators or inhibitors, respectively (Fig. 7A–D). Here, p-ERK activators or inhibitors considerably stimulated or impaired tubule formation (Fig. 7E–G), indicating that RhoC/ROCK2 promotes VM partly *via* ERK/MMP signaling. Moreover, higher FAK activity promotes VM and metastasis in malignant melanoma cells [41] and facilitates angiogenesis in astrocytic tumors [42]. Our results showed that p-FAK and p-paxillin levels increased remarkably following overexpression of RhoC (Fig. 7A) but were only slightly affected after knockdown of ROCK2 (Fig. 7B), which indicated that RhoC affects FAK, but not through ROCK2. Furthermore, the expression of MMP9 did not vary according to different changes in the expression of RhoC or ROCK2 (Fig. 7A, B), consistent with previous research [16]. Our results indicate that RhoC/ROCK2 is able to regulate these processes in HCC partly through ERK/MMPs signaling.

In the current study, we demonstrated the role of RhoC and differentiated the function of ROCK1 and ROCK2 in VM in HCC cells. Our study suggested that RhoC overexpression might lead to poor prognosis *via* promoting VM that could be induced by an EMT mechanism. Compared to ROCK1, ROCK2 may have a broader function, and its knockdown results in a more significant downregulation in the expression of key factors involved in VM, leading to the successful suppression of VM. According to the results above, we now hypothesize that highly activated RhoC/ROCK2 elevated VE-cadherin and MMP2 expression and raised the occurrence of EMT *via* activating ERK/MMPs signaling, which ultimately promoted VM formation (Fig. 8).

Supplementary data to this article can be found online at https://doi.org/10.1016/j.bbadis.2018.12.007.

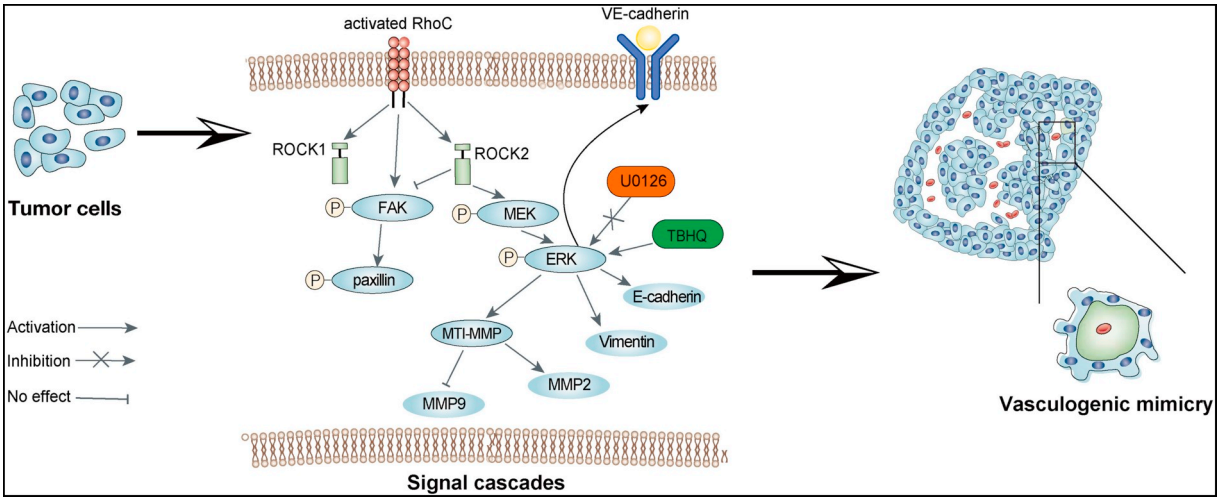

Fig. 8. Schematic form of the proposed mechanisms of the effect of RhoC/ROCK2 on VM formation. The highly activated RhoC/ROCK2 elevated VE-cadherin and MMP2 expression and raised the occurrence of EMT *via* activating ERK/MMPs signaling, which ultimately promoted VM formation.

Competing interests

The authors have declared that no competing interests exist.

Transparency Document

The Transparency document associated with this article can be found in the online version.

Acknowledgments

This work was supported by grants from the National Natural Science Foundation of China (NSFC, No.81572449 and No.81602524); sponsored by the Interdisciplinary Program of Shanghai Jiao Tong University (No.YG2015QN18).

References

[1] T. Chiba, E. Suzuki, T. Saito, S. Ogasawara, Y. Ooka, A. Tawada, A. Iwama, O. Yokosuka, Biological features and biomarkers in hepatocellular carcinoma, World J. Hepatol. 7 (2015) 2020–2028.
[2] K. Schutte, M. Kipper, S. Kahl, J. Bornschein, T. Gotze, D. Adolf, J. Arend, R. Seidensticker, H. Lippert, J. Ricke, P. Malfertheiner, Clinical characteristics and time trends in etiology of hepatocellular cancer in Germany, Digestion 87 (2013) 147–159.
[3] B. Njei, Y. Rotman, I. Ditah, J.K. Lim, Emerging trends in hepatocellular carcinoma incidence and mortality, Hepatology 61 (2015) 191–199.
[4] S. Mittal, H.B. El-Serag, Epidemiology of hepatocellular carcinoma: consider the population, J. Clin. Gastroenterol. 47 (2013).
[5] D. Sun, B. Sun, T. Liu, X. Zhao, N. Che, Q. Gu, X. Dong, Z. Yao, R. Li, J. Li, J. Chi, R. Sun, Slug promoted vasculogenic mimicry in hepatocellular carcinoma, J. Cell. Mol. Med. 17 (2013) 1038–1047.
[6] J.L. Ma, S.X. Han, Q. Zhu, J. Zhao, D. Zhang, L. Wang, Y. Lv, Role of Twist in vasculogenic mimicry formation in hypoxic hepatocellular carcinoma cells in vitro, Biochem. Biophys. Res. Commun. 408 (2011) 686–691.
[7] C.C. Wong, C.M. Wong, S.L. Au, I.O. Ng, RhoGTPases and Rho-effectors in hepatocellular carcinoma metastasis: ROCK N'Rho move it, Liver Int. 30 (2010) 642–656.
[8] N. Kaushal, Y.Y. Durmaz, L. Bao, S.D. Merajver, M.E. ElSayed, "Smart" nanoparticles enhance the cytoplasmic delivery of anti-RhoC silencing RNA and inhibit the migration and invasion of aggressive breast cancer cells, Mol. Pharm. 12 (2015) 2406–2417.
[9] Z. Cao, M. Bao, L. Miele, F.H. Sarkar, Z. Wang, Q. Zhou, Tumour vasculogenic mimicry is associated with poor prognosis of human cancer patients: a systemic review and meta-analysis, Eur. J. Cancer 49 (2013) 3914–3923.
[10] T. Kamai, T. Yamanishi, H. Shirataki, K. Takagi, H. Asami, Y. Ito, K.-I. Yoshida, Overexpression of RhoA, Rac1, and Cdc42 GTPases is associated with progression in testicular cancer, Clin. Cancer Res. 10 (2004) 4799–4805.
[11] T. Kamai, T. Tsujii, K. Arai, K. Takagi, H. Asami, Y. Ito, H. Oshima, Significant association of rho/ROCK pathway with invasion and metastasis of bladder cancer, Clin. Cancer Res. 9 (2003) 2632–2641.
[12] Y. Shimizu, D. Thumkeo, J. Keel, T. Ishizaki, H. Oshima, M. Oshima, Y. Noda, F. Matsumura, M.M. Taketo, S. Narumiya, ROCK-I regulates closure of the eyelids and ventral body wall by inducing assembly of actomyosin bundles, J. Cell Biol. 168 (2005) 941–953.
[13] D. Thumkeo, J. Keel, T. Ishizaki, M. Hirose, K. Nonomura, H. Oshima, M. Oshima, M.M. Taketo, S. Narumiya, Targeted disruption of the mouse rho-associated kinase 2 gene results in intrauterine growth retardation and fetal death, Mol. Cell. Biol. 23 (2003) 5043–5055.
[14] B.A. Bryan, E. Dennstedt, D.C. Mitchell, T.E. Walshe, K. Noma, R. Loureiro, M. Saint-Geniez, J.-P. Campaigniac, J.K. Liao, P.A. D'Amore, RhoA/ROCK signaling is essential for multiple aspects of VEGF-mediated angiogenesis, FASEB J. 24 (2010) 3186–3195.
[15] S.Y. Leong, C.H. Faux, A. Turbic, K.J. Dixon, A.M. Turnley, The Rho kinase pathway regulates mouse adult neural precursor cell migration, Stem Cells 29 (2011) 332–343.
[16] J.-G. Zhang, X.-Y. Li, Y.-Z. Wang, Q.-D. Zhang, S.-Y. Gu, X. Wu, G.-H. Zhu, Q. Li, G.-L. Liu, ROCK is involved in vasculogenic mimicry formation in hepatocellular carcinoma cell line, PLoS One 9 (2014) e107661.
[17] M.J. Hendrix, E.A. Seftor, P.S. Meltzer, L.M. Gardner, A.R. Hess, D.A. Kirschmann, G.C. Schatteman, R.E. Seftor, Expression and functional significance of VE-cadherin in aggressive human melanoma cells: role in vasculogenic mimicry, Proc. Natl. Acad. Sci. U. S. A. 98 (2001) 8018–8023.
[18] R.E. Seftor, E.A. Seftor, N. Koshikawa, P.S. Meltzer, L.M. Gardner, M. Bilban, W.G. Stetler-Stevenson, V. Quaranta, M.J. Hendrix, Cooperative interactions of laminin 5 γ2 chain, matrix metalloproteinase-2, and membrane type-1-matrix/metalloproteinase are required for mimicry of embryonic vasculogenesis by aggressive melanoma, Cancer Res. 61 (2001) 6322–6327.
[19] J.P. Thiery, Epithelial–mesenchymal transitions in tumour progression, Nat. Rev. Cancer 2 (2002) 442–454.
[20] X. Liu, J.H. Wang, S. Li, L.L. Li, M. Huang, Y.H. Zhang, Y. Liu, Y.T. Yang, R. Ding, Y.Q. Ke, Histone deacetylase 3 expression correlates with vasculogenic mimicry through the phosphoinositide3-kinase/ERK-MMP-laminin5gamma2 signaling pathway, Cancer Sci. 106 (2015) 857–866.
[21] M. Zang, Y. Zhang, B. Zhang, L. Hu, J. Li, Z. Fan, H. Wang, L. Su, Z. Zhu, C. Li, C. Yan, Q. Gu, B. Liu, M. Yan, CEACAM6 promotes tumor angiogenesis and vasculogenic mimicry in gastric cancer via FAK signaling, Biochim. Biophys. Acta 1852 (2015) 1020–1028.
[22] T. Smutny, M. Bitman, M. Urban, M. Dubecka, R. Vrzal, Z. Dvorak, P. Pavek, U0126, a mitogen-activated protein kinase kinase 1 and 2 (MEK1 and 2) inhibitor, selectively up-regulates main isoforms of CYP3A subfamily via a pregnane X receptor (PXR) in HepG2 cells, Arch. Toxicol. 88 (2014) 2243–2259.
[23] R. Yu, T.H. Tan, A.N. Kong, Butylated hydroxyanisole and its metabolite tert-butylhydroquinone differentially regulate mitogen-activated protein kinases. The role of oxidative stress in the activation of mitogen-activated protein kinases by phenolic antioxidants, J. Biol. Chem. 272 (1997) 28962–28970.
[24] D.A. Kirschmann, E.A. Seftor, K.M. Hardy, R.E. Seftor, M.J. Hendrix, Molecular pathways: vasculogenic mimicry in tumor cells: diagnostic and therapeutic implications, Clin. Cancer Res. 18 (2012) 2726–2732.
[25] S.Y. Wang, L. Yu, G.Q. Ling, S. Xiao, X.L. Sun, Z.H. Song, Y.J. Liu, X.D. Jiang, Y.Q. Cai, Y.Q. Ke, Vasculogenic mimicry and its clinical significance in medulloblastoma, Cancer Biol. Ther. 13 (2012) 341–348.
[26] J.Y. Zhang, H.S. Dong, R.K. Oqani, T. Lin, J.W. Kang, D. Il Jin, Distinct roles of ROCK1 and ROCK2 during development of porcine preimplantation embryos, Reproduction 1 (2014) 99–107.
[27] B. Sommer, L.M. Montano, J. Chavez, V. Carbajal, L.M. Garcia-Hernandez, C. Irles, A.M. Jimenez-Garduno, A. Ortega, ROCK1 translocates from non-caveolar to caveolar regions upon KCl stimulation in airway smooth muscle, Physiol. Res. 2 (2014) 179–187.
[28] J. Shi, X. Wu, M. Surma, S. Vemula, L. Zhang, Y. Yang, R. Kapur, L. Wei, Distinct

roles for ROCK1 and ROCK2 in the regulation of cell detachment, Cell Death Dis. 4 (2013) e483.
[29] M. Iizuka, K. Kimura, S. Wang, K. Kato, M. Amano, K. Kaibuchi, A. Mizoguchi, Distinct distribution and localization of Rho-kinase in mouse epithelial, muscle and neural tissues, Cell Struct. Funct. 37 (2012) 155–175.
[30] B. Sun, S. Zhang, D. Zhang, J. Du, H. Guo, X. Zhao, W. Zhang, X. Hao, Vasculogenic mimicry is associated with high tumor grade, invasion and metastasis, and short survival in patients with hepatocellular carcinoma, Oncol. Rep. 16 (2006) 693–698.
[31] A. Hakem, O. Sanchez-Sweatman, A. You-Ten, G. Duncan, A. Wakeham, R. Khokha, T.W. Mak, RhoC is dispensable for embryogenesis and tumor initiation but essential for metastasis, Genes Dev. 19 (2005) 1974–1979.
[32] X.D. Xu, H.B. Shen, L. Zhu, J.Q. Lu, L. Zhang, Z.Y. Luo, Y.Q. Wu, Anti-RhoC siRNAs inhibit the proliferation and invasiveness of breast cancer cells via modulating the KAI1, MMP9, and CXCR4 expression, Onco Targets Ther. 10 (2017) 1827–1834.
[33] R.E.B. Seftor, A.R. Hess, E.A. Seftor, D.A. Kirschmann, K.M. Hardy, N.V. Margaryan, M.J.C. Hendrix, Tumor cell vasculogenic mimicry: from controversy to therapeutic promise, Am. J. Pathol. 181 (2012) 1115–1125.
[34] Y.L. Fan, M. Zheng, Y.L. Tang, X.H. Liang, A new perspective of vasculogenic mimicry: EMT and cancer stem cells (review), Oncol. Lett. 6 (2013) 1174–1180.
[35] X. Lu, H. Guo, X. Chen, J. Xiao, Y. Zou, W. Wang, Q. Chen, Effect of RhoC on the epithelial-mesenchymal transition process induced by TGF-beta1 in lung adenocarcinoma cells, Oncol. Rep. 36 (2016) 3105–3112.
[36] J.Q. Guo, Q.H. Zheng, H. Chen, L. Chen, J.B. Xu, M.Y. Chen, D. Lu, Z.H. Wang, H.F. Tong, S. Lin, Ginsenoside Rg3 inhibition of vasculogenic mimicry in pancreatic cancer through downregulation of VEcadherin/EphA2/MMP9/MMP2 expression, Int. J. Oncol. 45 (2014) 1065–1072.
[37] Q. Huang, F. Lan, X. Wang, Y. Yu, X. Ouyang, F. Zheng, J. Han, Y. Lin, Y. Xie, F. Xie, W. Liu, X. Yang, H. Wang, L. Dong, L. Wang, J. Tan, IL-1beta-induced activation of p38 promotes metastasis in gastric adenocarcinoma via upregulation of AP-1/c-fos, MMP2 and MMP9, Mol. Cancer 13 (2014) 18.
[38] W. Zhu, W. Sun, J.T. Zhang, Z.Y. Liu, X.P. Li, Y.Z. Fan, Norcantharidin enhances TIMP2 antivasculogenic mimicry activity for human gallbladder cancers through downregulating MMP2 and MT1MMP, Int. J. Oncol. 46 (2015) 627–640.
[39] R.E. Seftor, E.A. Seftor, N. Koshikawa, P.S. Meltzer, L.M. Gardner, M. Bilban, W.G. Stetler-Stevenson, V. Quaranta, M.J. Hendrix, Cooperative interactions of laminin 5 gamma2 chain, matrix metalloproteinase-2, and membrane type-1-matrix/metalloproteinase are required for mimicry of embryonic vasculogenesis by aggressive melanoma, Cancer Res. 61 (2001) 6322–6327.
[40] A.R. Hess, E.A. Seftor, R.E.B. Seftor, M.J.C. Hendrix, Phosphoinositide 3-kinase regulates membrane type 1-matrix metalloproteinase (MMP) and MMP-2 activity during melanoma cell vasculogenic mimicry, Cancer Res. 63 (2003) 4757–4762.
[41] D.A. Ucar, L.H. Dang, S.N. Hochwald, Focal adhesion kinase signaling and function in pancreatic cancer, Front. Biosci. (Elite Ed.) 3 (2011) 750–756.
[42] H. Haskell, M. Natarajan, T.P. Hecker, Q. Ding, J. Stewart Jr., J.R. Grammer, C.L. Gladson, Focal adhesion kinase is expressed in the angiogenic blood vessels of malignant astrocytic tumors in vivo and promotes capillary tube formation of brain microvascular endothelial cells, Clin. Cancer Res. 9 (2003) 2157–2165.